Hindawi Publishing Corporation
Mathematical Problems in Engineering
Volume 2013, Article ID 754782, 8 pages
http://dx.doi.org/10.1155/2013/754782

Research Article

The Flow of a Variable Viscosity Fluid down an Inclined Plane with a Free Surface

M. S. Tshehla

Department of Mathematics, Faculty of Military Science, University of Stellenbosch, Private Bag X2, Saldanha 7395, South Africa

Correspondence should be addressed to M. S. Tshehla; samuel@ma2.sun.ac.za

Received 17 June 2013; Accepted 14 August 2013

Academic Editor: Oluwole Daniel Makinde

The effect of a temperature dependent variable viscosity fluid flow down an inclined plane with a free surface is investigated. The fluid film is thin, so that lubrication approximation may be applied. Convective heating effects are included, and the fluid viscosity decreases exponentially with temperature. In general, the flow equations resulting from the variable viscosity model must be solved numerically. However, when the viscosity variation is small, then an asymptotic approximation is possible. The full solutions for the temperature and velocity profiles are derived using the Runge-Kutta numerical method. The flow controlling parameters such as the nondimensional viscosity variation parameter, the Biot and the Brinkman numbers, are found to have a profound effect on the resulting flow profiles.

1. Introduction

The study of the flow of a viscous fluid with temperature dependent properties is of great importance in industries such as food processing, coating, and polymer processing, see Macosko and Oron et al. [1, 2]. In industrial systems fluids can be subjected to extreme conditions such as high temperature, pressure, and shear rates. External heating such as the ambient temperature and high shear rates can lead to a high temperature being generated within the fluid. This may have a significant effect on the fluid properties. It is a well-known fact in fluid dynamics studies that the property which is most sensitive to temperature rise is viscosity, see Myers et al. [3]. Fluids used in industries such as polymer fluids have a viscosity that varies rapidly with temperature and this may give rise to strong feedback effects, which can lead to significant changes in the flow structure of the fluid, see Wyle and Huang [4]. Due to the strong coupling effect between the Navier-Stokes and energy equations, viscous heating also plays an important role in fluids with strong temperature dependence, see Costa and Macedonio [5]. In this paper we focus on the effect of temperature on the viscosity. In particular, we investigate the viscosity variation by Reynolds law [5] or Nahme's law [3], which assumes that the viscosity varies exponentially with temperature. Myers et al. [3] studied the flow of variable viscosity between parallel plates with shear heating. Costa and Macedonio [5] applied the temperature dependent viscosity model to study magma flows. Elbashbeshy and Bazid [6] investigated the effect of temperature dependent viscosity on heat transfer over a moving surface. In their investigation, the fluid viscosity model varies as an inverse linear function of temperature. The work in [6] was extended in [7] to include variable internal heat generation. The solution was obtained using the Runge-Kutta numerical method, and results presented show that when the coefficient of viscosity variation parameter increases, the temperature of the fluid (water) increases slightly, whilst the opposite is true for the velocity profiles. Elbarbary and Elgazery [8] investigated the effects of variable viscosity and variable thermal conductivity on heat transfer from moving surfaces with radiation. In their work the fluid viscosity also varies as an inverse linear function of temperature, and the thermal conductivity varies as a linear function of temperature. The effect of convective heat transfer is extremely important in understanding the flow structure of many fluids used in industrial and natural applications. The present paper is aimed at investigating the effect of convective heat transfer on the flow of a viscous fluid with exponential temperature dependent viscosity, down an inclined plane with a free surface.

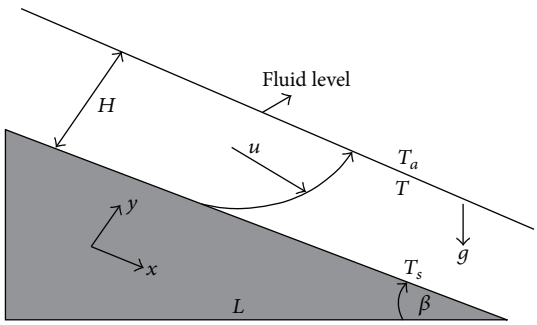

Figure 1: The geometry of the problem.

2. Problem Formulation

Figure 1 represents a two-dimensional laminar flow with a free surface. The figure depicts an infinitely wide channel of typical length scale L in the x direction and height H in the y direction. The fluid flows down a plane inclined at an angle β, and the dominant driving force for the flow is gravity, denoted g. The ambient temperature is denoted T_a, the fluid temperature is denoted T, and the temperature at the bottom surface is denoted T_s. The fluid viscosity μ will not be specified, but the viscosity of the fluid will vary exponentially with temperature.

In developing the mathematical model for the fluid flow, the following assumptions will be made:

(i) the fluid is incompressible, but the viscosity, $\mu(T)$, is temperature dependent;

(ii) the governing equations are derived for a thin film flow such that lubrication theory may be applied;

(iii) the film height T is considered to be constant;

(iv) the flow regime is laminar.

Taking into account these assumptions, the continuity, Navier-Stokes, and energy equations are written as follows:

$$\frac{\partial u}{\partial x}+\frac{\partial v}{\partial y}=0,$$

$$\rho\left(\frac{\partial u}{\partial t}+u\frac{\partial u}{\partial x}+v\frac{\partial u}{\partial y}\right)=-\frac{\partial p}{\partial x}+\rho g\sin\beta+2\frac{\partial}{\partial x}\left(\mu\frac{\partial u}{\partial x}\right)+\frac{\partial}{\partial y}\left[\mu\left(\frac{\partial u}{\partial y}+\frac{\partial v}{\partial x}\right)\right],$$

$$\rho\left(\frac{\partial u}{\partial t}+u\frac{\partial v}{\partial x}+v\frac{\partial v}{\partial y}\right)=-\frac{\partial p}{\partial y}+\rho g\cos\beta+2\frac{\partial}{\partial y}\left(\mu\frac{\partial v}{\partial y}\right)+\frac{\partial}{\partial x}\left[\mu\left(\frac{\partial u}{\partial y}+\frac{\partial v}{\partial x}\right)\right],$$

$$\rho c_p\left(\frac{\partial T}{\partial t}+u\frac{\partial T}{\partial x}+v\frac{\partial T}{\partial y}\right)=k\left(\frac{\partial^2 T}{\partial x^2}+\frac{\partial^2 T}{\partial y^2}\right)+\left[\frac{\partial p}{\partial t}+u\frac{\partial p}{\partial x}+v\frac{\partial p}{\partial y}\right]+\mu\left[2\left(\frac{\partial u}{\partial x}\right)^2+\left(\frac{\partial u}{\partial x}+\frac{\partial v}{\partial y}\right)^2+2\left(\frac{\partial v}{\partial y}\right)^2\right],\tag{1}$$

where the notation is defined in the nomenclature showed at the end of the paper. These governing equations are nondimensionalised using the following scales:

$$x=Lx',\qquad y=Hy',\qquad u=Uu',\qquad v=\frac{HU}{L}v',\qquad t=\frac{L}{U}t',\qquad \mu=\mu_0\mu'\,p=Pp'=\frac{\mu_{0UL}}{H^2}p',\qquad T=T_0+(T_a-T_0)\,T'=T_0+\Delta TT',\tag{2}$$

where all quantities with prime denote nondimensional parameters. The pressure scale $P=\mu_0UL/H^2$ is standard for lubrication theory. The reference viscosity and the temperature difference are denoted by μ_0 and ΔT, respectively. To simplify notation, the primes are omitted from now on. Since the film is thin, the aspect ratio $\varepsilon=H/L\ll 1$. Using the scaled parameters, (1) now becomes

$$\frac{\partial u}{\partial x}+\frac{\partial v}{\partial y}=0,$$

$$\varepsilon^2\,\mathrm{Re}\left(\frac{\partial u}{\partial t}+u\frac{\partial u}{\partial x}+v\frac{\partial u}{\partial y}\right)=-\frac{\partial p}{\partial x}+1+2\varepsilon^2\frac{\partial}{\partial x}\left(\mu\frac{\partial u}{\partial x}\right)+\frac{\partial}{\partial y}\left[\mu\left(\frac{\partial u}{\partial y}+\varepsilon^2\frac{\partial v}{\partial x}\right)\right],$$

$$\varepsilon^2\mathrm{Re}^4\left(\frac{\partial u}{\partial t}+u\frac{\partial v}{\partial x}+v\frac{\partial v}{\partial y}\right)=-\frac{\partial p}{\partial y}+\varepsilon\cot\beta+2\varepsilon^2\frac{\partial}{\partial y}\left(\mu\frac{\partial v}{\partial y}\right)+\varepsilon^2\frac{\partial}{\partial x}\left[\mu\left(\frac{\partial u}{\partial y}+\varepsilon^2\frac{\partial v}{\partial x}\right)\right],$$

$$\varepsilon^2\mathrm{Pe}\left(\frac{\partial T}{\partial t}+u\frac{\partial T}{\partial x}+v\frac{\partial T}{\partial y}\right)=\varepsilon^2\frac{\partial^2 T}{\partial x^2}+\frac{\partial^2 T}{\partial y^2}+\mathrm{Pr\,Ec}\left[\frac{\partial p}{\partial t}+u\frac{\partial p}{\partial x}+v\frac{\partial p}{\partial y}\right]+\Phi,\tag{3}$$

where

$$\Phi=\mathrm{Br}\mu\left[2\varepsilon^2\left(\frac{\partial u}{\partial x}\right)^2+2\varepsilon^2\left(\frac{\partial v}{\partial y}\right)^2+\left(\frac{\partial u}{\partial y}+\varepsilon^2\frac{\partial v}{\partial x}\right)^2\right].\tag{4}$$

The Péclet number $\mathrm{Pe} = \rho c_p UL/k$ represents the ratio of convective heat transport to the conductive heat transport, and the Brinkman number $\mathrm{Br} = \mu_0 U^2/k\Delta T$ represents the ratio of heat dissipation to fluid conduction. The Prandtl number $\mathrm{Pr} = \mu_0 c_p/k$ denotes the ratio of diffusivity for momentum to thermal diffusivity. The Eckert number $\mathrm{Ec} = U^2/c_p T_0$ denotes the ratio of kinetic energy to thermal mass. The velocity scale is given by $U = \rho g H^2 \sin\beta/\mu_0$, which denotes the ratio of gravitational forces to the dynamic viscosity. The parameter values may vary widely depending on the particular industrial application or the models under investigation. The parameter values for a lubricant are

$$\begin{gathered} \mu_0 \sim 10^{-3}\text{–}0.5\,\mathrm{kg/ms}, \qquad c_p \sim 2000\,\mathrm{J/kgK}, \\ H \sim 10^{-3}\,\mathrm{m}, \qquad k \sim 0.13\,\mathrm{W/mK}, \\ K_c \sim 10^{3}, \qquad L \sim 0.005, \\ \varepsilon \sim 10^{-4}, \qquad \rho \sim 880\text{–}940\,\mathrm{kg/m^3}. \end{gathered} \tag{5}$$

The experimental values listed above are taken from several references, [9, page 4], and [10–13]. Using these values listed above, we obtain

$$\begin{gathered} \mathrm{Br} = \frac{\mu_0 U^2}{k\Delta T} \sim 0.01\text{–}0.5, \qquad \mathrm{Pe} = \frac{\rho c_p UL}{k} \sim 10^5, \\ \mathrm{PrEc} = \frac{\mu_0 U^2}{kT_0} \sim 5 \times 10^{-4}, \\ \mathrm{Re} = \frac{\rho UL}{\mu_0} \sim 40\text{–}2000, \\ U = \frac{\rho g H^2 \sin 30}{\mu_0} \sim 0.4\,\mathrm{m/s}. \end{gathered} \tag{6}$$

Despite the fact that the Péclet number is large, the reduced Péclet number $\varepsilon^2\mathrm{Pe} \approx 10^{-3}$ is small and may be neglected in the governing equations. The reduced Reynolds number $\varepsilon^2\,\mathrm{Re} \approx 1.8 \times 10^{-5}$ may also be neglected. The reduced quantity PrEc is also assumed to be small, so it will be neglected from the governing equations. The Brinkman number may be close to unity and so must be retained. Using the above approximations, (3) may now be reduced to their final form:

$$\frac{\partial u}{\partial x} + \frac{\partial v}{\partial y} = 0, \tag{7}$$

$$-\frac{\partial p}{\partial x} + \frac{\partial}{\partial y}\left[\mu\left(\frac{\partial u}{\partial y}\right)\right] + 1 = 0 + \mathcal{O}\left(\varepsilon^2, \varepsilon^2\,\mathrm{Re}\right), \tag{8}$$

$$-\frac{\partial p}{\partial y} + \varepsilon\cot\beta = 0 + \mathcal{O}\left(\varepsilon^2, \varepsilon^4\,\mathrm{Re}\right), \tag{9}$$

$$\frac{\partial^2 T}{\partial y^2} + \mu\mathrm{Br}\left(\frac{\partial u}{\partial y}\right)^2 = 0 + \mathcal{O}\left(\varepsilon^2, \varepsilon^2\mathrm{Pe}\right). \tag{10}$$

The velocity and the temperature profiles may be determined after the boundary conditions associated with (7)–(10) are stated.

3. Boundary Conditions

(i) At $y = 0$, a no slip boundary condition is applied, and the temperature at the bottom surface is constant:

$$u(0) = v(0) = 0, \qquad T(0) = 0. \tag{11}$$

(ii) At the free surface, the shear stress is zero and the fluid temperature is imposed by the air and substrate, respectively:

$$\left(\frac{\partial u}{\partial y}\right)\Big|_{y=h} = 0, \qquad \left(\frac{\partial T}{\partial y}\right)\Big|_{y=h} = \mathrm{Bi}\,(T-1), \tag{12}$$

where $\mathrm{Bi} = HK_c/k$ is the Biot number and denotes the ratio of heat transfer to thermal conductivity, Alhama and Zueco [14] and Makinde [15]. The parameters k and K_c denote the thermal conductivity and heat transfer coefficient, respectively. The fluid at the free surface is exposed to the ambient temperature. Hence, a cooling condition is applied.

In the following section the variable viscosity model is introduced, and the equations governing the flow are coupled to this model and solved using both analytical and numerical methods.

4. Variable Viscosity Analysis

We now focus on the fluid with an exponential variation of the form:

$$\mu = \mu_0 e^{-\theta(T-T_0)}, \tag{13}$$

where μ_0 is the reference viscosity at the reference temperature T_0 and θ is the coefficient of viscosity variation with temperature Costa and Macedonio [5]. Equation (13) can be written in nondimensional form,

$$\mu = e^{\propto T}, \tag{14}$$

where $\propto = \theta\Delta T$. Equation (14) is commonly known as Nahme's exponential law [5] or Reynolds law, see Myers et al. [3]. Combining (8) and (14), integrating with respect to y, and applying the boundary conditions (12) give the velocity gradient,

$$\frac{\partial u}{\partial y} = (1-y)\,e^{\propto T}, \tag{15}$$

where we have used the fact that $\partial p/\partial x = 0$ to write (15) as a result from (9). Equation (15) cannot be integrated further to determine u, since it involves the temperature T which is unknown, so it must be solved numerically using the Runge-Kutta method. Substituting (14) and (15) into the reduced energy (10) gives

$$\frac{\partial^2 T}{\partial y^2} = \mathrm{Br}(1-y)^2 e^{\alpha T}. \tag{16}$$

Equations (15) and (16) form a coupled system of nonlinear partial differential equations which require a numerical technique to obtain a full solution. However, when the viscosity variation is gradual, that is, $\alpha \ll 1$ and $T \sim \mathcal{O}(1)$, an asymptotic analysis is possible. The main reason for using an asymptotic analysis is that we can clearly illustrate how the parameters affect the flow by looking into the dominant terms from the governing equations. This approach can be used to validate numerics. The question is how small must the parameter α be? Therefore, the key factor in determining the stage at which $\propto$ is small is the magnitude of ΔT, since θ is the fluid property. In certain industrial applications for lubricating oil, the experimental values for the temperature may be confined in the region $50\,^{\circ}\mathrm{C} \le T \le 300\,^{\circ}\mathrm{C}$; see [12, 13, 16], for example. Our interest is on large values ΔT, since $\propto \sim \theta \Delta T$, and usually the fluid property θ for lubricant is small. Now taking the temperature difference $\Delta T \sim 200\,^{\circ}\mathrm{C}$ and $\theta \sim 0.00242$ (see [17, page 31]), it can easily be shown that $\propto \sim 0.5$ for a lubricating oil. It is important to note that for different values of θ and ΔT, the results will obviously yield a different value of $\propto$, depending on the fluid under investigation. The velocity and temperature may then be expanded in a series form,

$$u = u_0 + \propto u_1, \tag{17}$$

$$T = T_0 + \propto T_1, \tag{18}$$

where u_0, T_0, u_1, and T_1 represent the leading-order terms and the first-order perturbation terms in $\propto$. Substituting for T into (16) yields

$$\frac{\partial^2 T_0}{\partial y^2} + \propto \frac{\partial^2 T_1}{\partial y^2} = -\mathrm{Br}(1-y)^2 - \propto T_0 (1-y)^2 . \tag{19}$$

The leading order and $\mathcal{O}(\propto)$ terms from (19) are

$$\frac{\partial^2 T_0}{\partial y^2} = -\mathrm{Br}(1-y)^2, \tag{20}$$

$$\frac{\partial^2 T_1}{\partial y^2} = -\mathrm{Br}(1-y)^2. \tag{21}$$

Equations (20) and (21) are solved subject to

$$T_0 = T_1 = 0 \quad \text{at } y = 0, \qquad \left(\frac{\partial T_0}{\partial y}\right)\Big|_{y=1} = -\mathrm{Bi}\ (T_0 - 1), \qquad \left(\frac{\partial T_1}{\partial y}\right)\Big|_{y=1} = \mathrm{Bi}\ T_1. \tag{22}$$

Integrating (21) with respect to y and applying the boundary conditions in (22) yield

$$T_0 = -\frac{\mathrm{Br}}{12}\left[(1-y)^4 - \left(1 - \frac{\mathrm{Bi}}{(\mathrm{Bi}-1)}\right)\right] + \left(\frac{\mathrm{Bi}}{(\mathrm{Bi}-1)}\right) y. \tag{23}$$

Integrating Equation (21) and applying the boundary conditions (22), we obtain

$$\begin{aligned} T_1 = {} & \frac{\mathrm{Br}^2}{12}\left[\frac{1}{56}(1-y)^2 - \frac{1}{60}\left(5(1-y)^4 + \frac{\mathrm{Bi}}{(\mathrm{Bi}\ h=1)}\left(10y^3 - 10y^4 + 3y^5\right)\right)\right] \\ & + \frac{\mathrm{Br}^2}{12}\left[\frac{\mathrm{Bi}}{(\mathrm{Bi}-1)}\left(\frac{1}{12\,(\mathrm{Bi}-1)} - \frac{\mathrm{Bi}}{20\,(\mathrm{Bi}-1)}\right) y + \frac{11}{168}\right] + \frac{\mathrm{Bi}}{(\mathrm{Bi}-1)}\left(10y^3 - 10y^4 + 3y^5\right) \\ & + \frac{\mathrm{Bi}}{(\mathrm{Bi}-1)^2}\left(\frac{1}{12} - \frac{\mathrm{Bi}}{20}\right) y. \end{aligned} \tag{24}$$

The final temperature profile is obtained by combining both (23) and (24) as $= T_0 + \propto T_1$. Similarly, a solution for the velocity profile can be derived. Combining (15) and (17) gives

$$\frac{\partial u_0}{\partial y} + \alpha \frac{\partial u_1}{\partial y} = (1-y) + \propto T_a (1-y). \tag{25}$$

The leading order and $\mathcal{O}(\propto)$ terms are therefore

$$\frac{\partial u_0}{\partial y} = (1-y), \tag{26}$$

$$\frac{\partial u_1}{\partial y} = T_0 (1-y). \tag{27}$$

Equations (26) and (27) are solved subject to

$$u_0 = u_1 = 0 \quad \text{at } y = 0. \tag{28}$$

Equation (26) gives the Newtonian velocity profile as

$$u_0 = \frac{y}{2}(2-y). \tag{29}$$

A similar expression for (29) may be obtained in Myers et al. [3]. To obtain u_1, (23) and (27) are combined and integrated subject to (28),

$$\begin{aligned} u_1 = {} & -\frac{\mathrm{Br}}{72}\left[(1-y)^6 - 6\left(\left(\frac{y}{2}(2-y)\right) - \frac{\mathrm{Bi}\ y^2}{6\,(\mathrm{Bi}-1)}(3-2\ y)\right) - 1\right] \\ & + \frac{\mathrm{Bi}\ y^2}{6\,(\mathrm{Bi}-1)}(3-2y). \end{aligned} \tag{30}$$

The final velocity profile is given by (29) and (32) as $u = u_0 + \propto u_1$. The numerical solution is discussed in the following section.

5. Numerical Solution

The coupled nonlinear partial differential equations (15) and (16) for the velocity and the temperature profiles are solved numerically using the fourth-order Runge-Kutta integration scheme. The solution for the temperature profile must be calculated first and then substituted into the velocity equation to obtain the solution for the velocity profile. Setting $t_1 = T$ and $t_2 = \partial T/\partial y$, (16) can be written as a system of two first-order equations in t_1 and t_2 of the form,

$$\frac{\partial}{\partial y}\begin{bmatrix} t_1 \\ t_2 \end{bmatrix} = \begin{bmatrix} t_2 \\ -\mathrm{Br}(1-y)^2 e^{\propto t_1} \end{bmatrix}. \tag{31}$$

This system can be written in vector form,

$$\frac{\partial \mathbf{t}}{\partial y} = F(\mathbf{t}, y), \tag{32}$$

where $\mathbf{t} = (t_1, t_2)$. The solutions for this system of differential equations are solved subject to the boundary conditions (11) and (12). The Runge-Kutta method requires an initial value, and the initial value for the temperature t_1 is taken as the boundary condition at $y = 0$. The corresponding initial value for t_2 is randomly chosen. It is important to note that the best numerical results largely depend on a good guess for the initial condition; see [6, 7]. Once this initial value is chosen, we employ the Runge-Kutta method to solve for the temperature. When the solution of the iterative process for the Runge-Kutta scheme terminates, then the derivative for the temperature t_2 at the free surface is eventually corrected using the given boundary conditions (12). The set of parameters $\propto$, Bi, and Br are coupled to the system of differential equations, and we solve our equations using a small step size for Δy. The velocity gradient is given by

$$\frac{\partial u}{\partial y} = (1-y)\, e^{\alpha t_1}. \tag{33}$$

Once the temperature profile is calculated, the velocity profile is computed from (32) using the finite difference scheme,

$$u_{n+1} = u_n + \Delta u_y \cdot \left(\frac{\partial u}{\partial y}\right)\Big|_{(y_i,\, t_i)}. \tag{34}$$

In Section 6, we will discuss the results for the asymptotic and numerical methods. We will give account of the findings in this paper. We proceed our analysis for comparison of the asymptotic and numerical solutions.

6. Results and Discussion

Figure 2 depicts a typical application of the temperature dependent model in (16). This illustrates the relations between temperatures of the fluid with the Brinkman number. This also is widely studied by several references, such as Myers et al. [3] who studied the application in a closed channel and Makinde [15, 18, 19] who investigated the application with a free surface flow. In this case, the critical point for the temperature is depicted at 0.53 after which the two solution branches are shown. When the temperature is greater than 0.53, the system has no real solution which is indicative of thermal runaway.

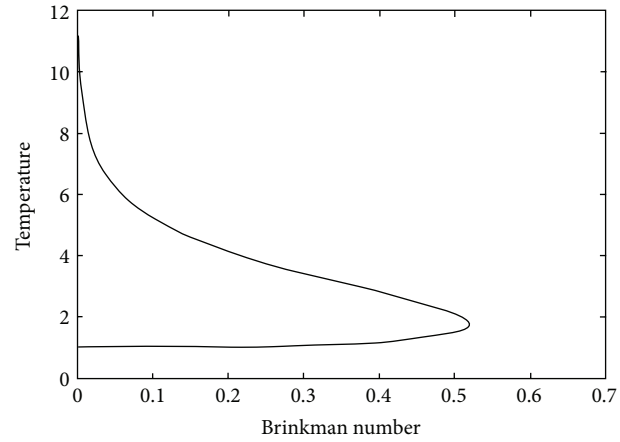

Figure 2: The channel temperature.

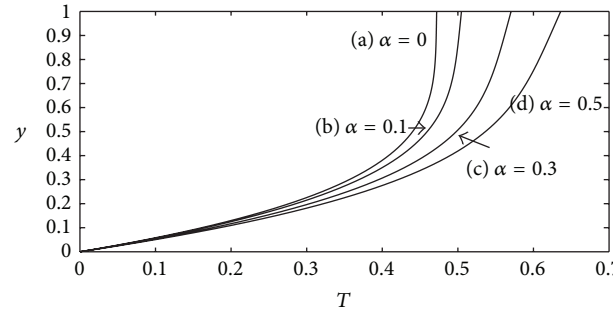

Figure 3: The temperature profiles for (18) and numerical solution.

Figure 3 shows the temperature profiles corresponding to (18) where T_0 and T_1 are given by (23) and (24) and the numerical solution. In this figure the dotted lines represent the profiles from the asymptotic solution and solid lines for the numerical solution. The results are calculated for the case Bi = Br = 0.3, so that the Biot and the Brinkman numbers are of the same magnitude. Different values of $\propto$ were considered in order to investigate its effect on resulting flow profiles. We start our investigation with a simple case where $\propto = 0$ for a Newtonian fluid to a maximum of $\propto = 0.5$ typically, for a lubricating oil. Curves (a), (b), (c), and (d) display four different values of $\propto$, namely, $\propto = 0, 0.1, 0.3$, and 0.5. It is important to note that when $\propto$ increases, the viscosity of the fluid decreases. The temperature of the fluid in all four curves increases to their maximum temperatures at the free surface. When $\propto$ increases, the temperature of the fluid increases due to heat generation by the internal friction caused by the collision of the fluid particles. The Newtonian case is retrieved in curve (a) with $\propto$. The numerical results are in good agreement with the asymptotic as shown in curves (a) through to (d). In Figure 4, four curves representing the velocity profiles for (17) where u_o and u_1 are given by (29) and (32) are plotted together with the numerical solution.

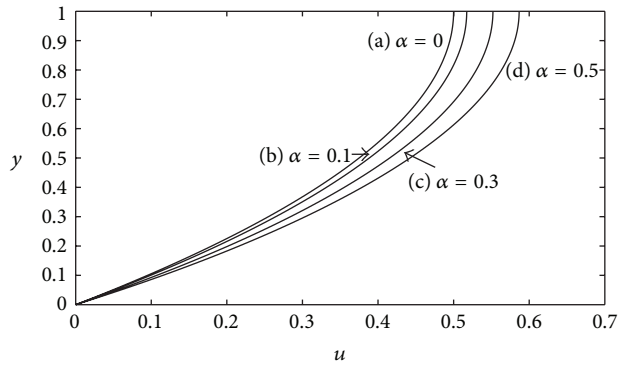

Figure 4: The velocity profile for (17) and numerical solution.

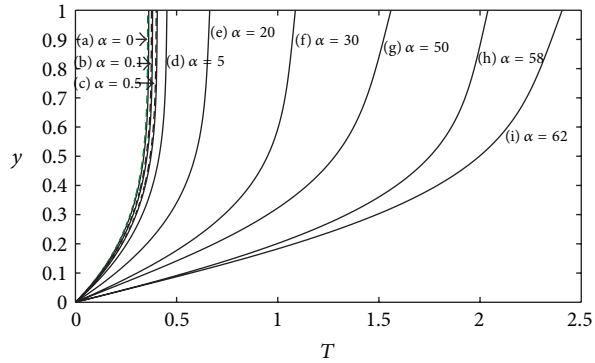

Figure 5: The temperature profiles for varying ∝.

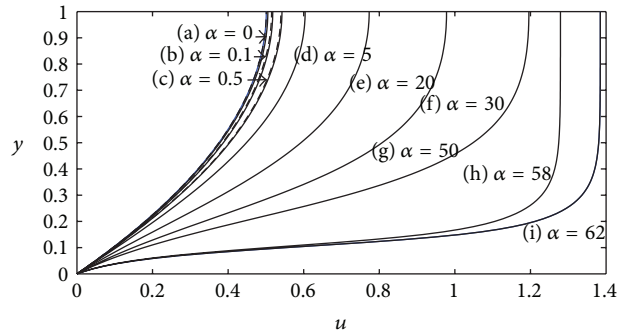

Figure 6: The velocity profiles for varying ∝.

These profiles correspond to different values of ∝ as shown in Figure 3. The figure shows that the velocity of the fluid increases when increases. This is a result of the resistance force to the flow which decreases as ∝ increases. Curve (a) displays a Newtonian velocity profile with ∝ = 0, and this curve increases across the fluid layer to the maximum point at the top due to the effect of the gravitational forces and lack of resistance force to the flow. As shown in the figure, the numerical and asymptotic velocity profiles are in good agreement, particularly for the set of curves (c) and (d).

In Figures 5 and 6 the temperature and the velocity profiles for a numerical solution are displayed. The profiles are plotted to include large values for ∝ as shown in curves (c) through to (h) from ∝ = 10 to 62 for the temperature profiles in Figure 5. The velocity gradient in (11) increases exponentially with temperature, which eventually feeds back into (12) through the viscous heating term. The Newtonian temperature profile is shown in curve (a) with ∝ = 0, and curve (b) is plotted with ∝ = 0.5; these curves are the same as the ones which are shown in Figure 3 curves (a) and (b). It is important to note that the large values of ∝ were randomly chosen to test the reliability of the numerical scheme. The resulting temperature profiles show that the temperature of the fluid increases significantly when ∝ increases. The velocity profiles are displayed in Figure 6. Curves (a) through to (f) correspond to different values of ∝ as displayed in the figure, and other flow controlling parameters are the same as those which are given in Figure 5. The velocity of the fluid for all these curves increases to the maximum velocity occurring at the free surface. In this case, when ∝ increases, the velocity of the fluid increases due to less resistance force to the flow. Curves (a) with ∝ = 0 and (b) with ∝ = 0.5 are similar to the ones shown in Figure 4. The resulting velocity profiles show that for values of ∝ > 50, a change in the flow structure is observed.

In Figure 6, curves (g) and (h) show different flow behaviour as compared to curves (a) through to (f). Since the viscosity of the fluid decreases exponentially when ∝ increases, this therefore causes the fluid to behave like a Newtonian fluid when ∝ = 58 and 62. Elbashbeshy and Bazid [6] analysed the effect of temperature dependent viscosity on heat transfer over a continuous moving surface. The full solutions for the velocity and temperature profiles were obtained using the fourth-order Runge-Kutta numerical scheme. Their results indicate that when the viscosity variation parameter increases for water, the temperature of the fluid increases slightly, which is in agreement with our results. However, in their investigation the velocity of the fluid decreases when the viscosity variation parameter increases.

The effect of the Biot number on the resulting temperature and velocity profiles is investigated. The importance of the Biot number is that it helps understand the influence of the ambient temperature on the flow system. When the Biot number tends to infinity ($k \to \infty$), then both the ambient temperature and the fluid temperature reache equilibrium and ~ 0. However, when the Biot number decreases ($k \to 0$), the fluid loses its temperature to the surrounding atmosphere, and this process will have a major influence on the temperature variation of the fluid. An increase in the Biot number indicates that more heat is lost from the fluid to the surrounding atmosphere (hence cooling the fluid). When the Biot number decreases, a reduction in heat transferred to the surrounding atmosphere occurs, and the fluid gets hotter [11]. Because of the strong feedback between the Navier-Stokes and the energy equations, the Biot number will have a major influence on the resulting velocity and temperature profiles. Using the parameters listed in the previous section, we can easily show that Bi = 7.692 ~ 8. We again begin with a simple analysis for Bi = 0 to a maximum of Bi = 8 calculated for lubricating oil. The curves for the temperature profiles are shown in Figure 7 with different values of the Biot numbers, namely, Bi = 0, 0.01, 1, 4, and 8. The fluid temperature increases across the fluid layer to its maximum temperatures at the free surface as Bi decreases due to reduction in the heat

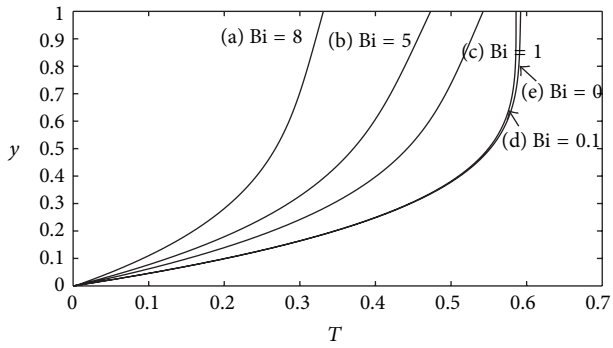

Figure 7: The temperature profiles for varying Bi.

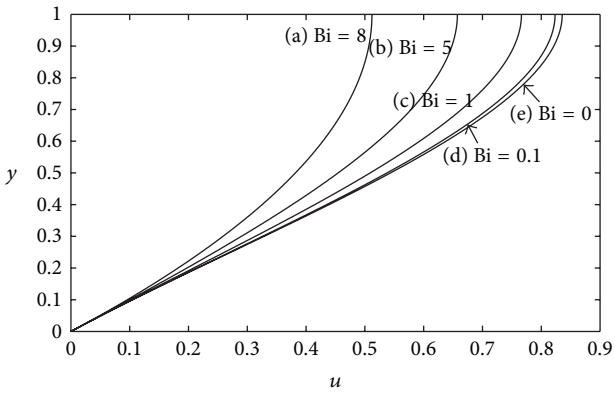

Figure 8: The velocity profiles for varying Bi.

transferred to the surrounding atmosphere. The figure clearly demonstrates that the fluid temperature rises with decreasing values of the Biot number, and the temperature profiles flatten out at the free surface as Bi decreases, and when Bi = 0, the temperature profile shows that the temperature gradient at the free surface is zero. Khaled [11] investigated the rate of heat and entropy transfer to the slab wall, and the results showed that the dimensionless temperature in the slab wall increases as Bi decreases, which is in agreement with our findings. The corresponding velocity profiles are shown in Figure 8 with different values of the Biot numbers. The fluid velocity increases across the layer to its maximum at the free surface as the Biot number decreases. This is a result of the resistance force to the flow which decreases as Bi decreases.

The effect of the Brinkman number is displayed in Figures 9 and 10 for the temperature and velocity profiles. Other parameters are given by $\alpha = 0.3$ and Bi = 0.3. Using the values listed in the previous section, the Brinkman numbers are given by Br = 0 for the Newtonian case to 0.5 as shown in Figure 9. We have the Newtonian case displayed in curves (a) in each figure with a constant viscosity. Increasing Br results in increased viscous heat dissipation effect. The temperature of the fluid increases significantly when Br increases. In Figure 9, when Br increases, the fluid heats up quickly, the viscosity of the fluid drops, and the flow is faster. As a result, the fluid velocity increases significantly in the direction of the flow.

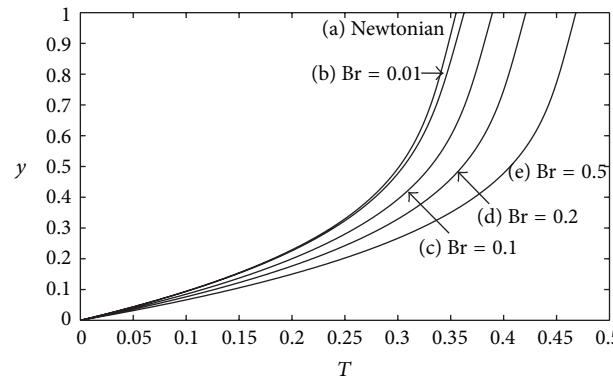

Figure 9: The effect of the Brinkman number on temperature profiles.

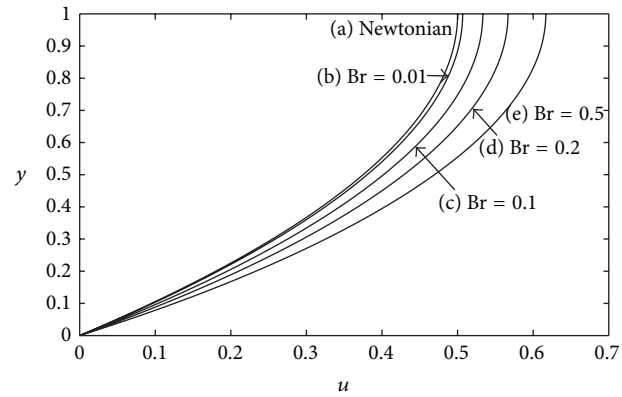

Figure 10: The effect of the Brinkman number on the velocity profiles.

7. Conclusion

A steady gravity driven flow of a temperature dependent variable viscosity model was investigated. The results were obtained using an asymptotic technique and the fourth-order Runge-Kutta integration scheme. We used experimental values for lubricating oil to determine the value of α for the asymptotic approximation terms. The numerical results were compared with the asymptotics. The Newtonian cases for both the temperature and velocity of the fluid are retrieved when α is zero, and the results showed good agreement in all the curves for the temperature and velocity profiles. The effects of large values of α on the resulting velocity and temperature profiles were further investigated. When α increase, the temperature and the velocity of the fluid increase significantly. However, when $\alpha = 58$, a change in the flow structure is observed from the velocity profiles. Since the viscosity of the fluid decreases exponentially when α increases, the prediction of the velocity profiles shows a different flow structure. This therefore causes the fluid to behave like a Newtonian fluid, in particular when $\alpha \geq 58$. Furthermore, the effect of the flow controlling parameters such as the Biot and the Brinkman numbers was investigated. In the case of the Biot number, the temperature of the fluid increases significantly when the Biot number decreases due

to heat lost from the fluid to the surrounding atmosphere, and as a result, the fluid temperature flattens out at the free surface. The velocity of the fluid increases as the Biot number decreases, due to less resistance force to the flow. The Brinkman number Br was also investigated, and the results showed that as Br increases, the temperature of the fluid increases due to heat dissipation, and the velocity of the fluid increased significantly due to the resistance force to the flow, which decreases when the Br increases.

Nomenclature

$\mathrm{Bi} = HK_c/k$:	Biot number
$\mathrm{Br} = \mu_{0U^2}/k\Delta T$:	Brinkman number
C_p:	Heat capacity ($\mathrm{J{\cdot}Kg^{-1}{\cdot}K^{-1}}$)
$\mathrm{Ec} = U^2/c_pT_0$:	Eckert number
g:	Acceleration due to gravity ($\mathrm{m\,s^2}$)
H:	Channel height (m)
k:	Thermal conductivity ($\mathrm{W{\cdot}m^{-1}{\cdot}K^{-1}}$)
K_c:	Heat transfer coefficient ($\mathrm{W{\cdot}m^{-2}{\cdot}K^{-1}}$)
L:	Channel length (m)
P:	Pressure scale (Pa)
p:	Pressure (Pa)
$\mathrm{Pe} = \rho c_pLU/k$:	Péclet number
$\mathrm{Pr} = \mu_0c_p/k$:	Prandtl number
$\mathrm{Re} = \rho UL/\mu_0$:	Renolds number
t:	Time (s)
T:	Temperature (°C)
T_a:	Ambient temperature (°C)
T_s:	Bottom surface temperature (°C)
ΔT:	Temperature drop (°C)
$U = \rho gH^2 \sin\beta/\mu_0$:	Velocity scale ($\mathrm{m\,s^1}$)
(u, v):	Cartesian velocity ($\mathrm{m\,s^1}$)
(x, y):	Cartesian coordinates (m)
ε:	Aspect ratio of the flow
μ:	Dynamic viscosity ($\mathrm{kg{\cdot}m^{-1}{\cdot}s^{-1}}$)
μ_0:	Dynamic viscosity reference ($\mathrm{kg{\cdot}m^{-1}{\cdot}s^{-1}}$)
Φ:	Viscous dissipation function
ρ:	Fluid density ($\mathrm{Kg{\cdot}m^{-3}}$)
θ:	Coefficient of viscosity variation ($\mathrm{K^{-1}}$).

References

[1] C. W. Macosko, *Rheology, Principles, Measurements, and Applications*, Wiley-VCH, Poughkeepsie, NY, USA, 1994.

[2] A. Oron, S. H. Davis, and S. G. Bankoff, "Long-scale evolution of thin liquid films," *Reviews of Modern Physics*, vol. 69, no. 3, pp. 931–980, 1997.

[3] T. G. Myers, J. P. F. Charpin, and M. S. Tshehla, "The flow of a variable viscosity fluid between parallel plates with shear heating," *Applied Mathematical Modelling*, vol. 30, no. 9, pp. 799–815, 2006.

[4] J. J. Wyle and H. Huang, "Extensional flows with viscous heating," *Journal of Fluid Mechanics*, vol. 571, pp. 359–370, 2007.

[5] A. Costa and G. Macedonio, "Viscous heating in fluids with temperature-dependent viscosity: implications for magma flows," *Nonlinear Processes in Geophysics*, vol. 10, no. 6, pp. 545–555, 2003.

[6] E. M. A. Elbashbeshy and M. A. A. Bazid, "The effect of temperature-dependent viscosity on heat transfer over a continuous moving surface," *Journal of Physics D*, vol. 33, no. 21, pp. 2716–2721, 2000.

[7] E. M. A. Elbashbeshy and M. A. A. Bazid, "The effect of temperature-dependent viscosity on heat transfer over a continuous moving surface with variable internal heat generation," *Applied Mathematics and Computation*, vol. 153, no. 3, pp. 721–731, 2004.

[8] E. M. E. Elbarbary and N. S. Elgazery, "Chebyshev finite difference method for the effects of variable viscosity and variable thermal conductivity on heat transfer from moving surfaces with radiation," *International Journal of Thermal Sciences*, vol. 43, no. 9, pp. 889–899, 2004.

[9] V. N. Constantinescu, *Laminar Viscous Flow*, Mechanical Engineering Series, Springer, New York, NY, USA, 1995.

[10] J. P. Holman, *Heat Transfer*, McGraw-Hill, New York, NY, USA, 6th edition, 1990.

[11] A.-R. A. Khaled, "Conduction heat and entropy transfer in a semi-infinite medium and wall with a combined periodic heat flux and convective boundary condition," *International Journal of Thermal Sciences*, vol. 47, no. 1, pp. 76–83, 2008.

[12] J. A. Schetz and A. E. Fuhs, *Fundamentals of Fluid Mechanics*, John Wiley & Sons, New York, NY, USA, 1999.

[13] F. M. White, *Fluid Mechanics*, McGraw-Hill, New York, NY, USA, 3rd edition, 1994.

[14] F. Alhama and J. Zueco, "Application of a lumped model to solids with linearly temperature-dependent thermal conductivity," *Applied Mathematical Modelling*, vol. 31, no. 2, pp. 302–310, 2007.

[15] O. D. Makinde, "Laminar falling liquid film with variable viscosity along an inclined heated plate," *Applied Mathematics and Computation*, vol. 175, no. 1, pp. 80–88, 2006.

[16] H. A. Barnes, J. F. Hutton, and K. Walters, *An Introduction to Rheology*, Elsevier, 1989.

[17] D. Knezevic and V. Savic, "Mathematical modelling of dynamic viscosity, as a function of temperature and pressure, of mineral oil for hydraulic systems," *Mechanical Engineering*, vol. 4, no. 1, pp. 27–34, 2006.

[18] O. D. Makinde, "Hermite-Padé approximation approach to steady flow of a liquid film with adiabatic free surface along an inclined heat plate," *Physica A*, vol. 381, no. 1-2, pp. 1–7, 2007.

[19] O. D. Makinde, "Thermal criticality for a reactive gravity driven thin film flow of a third-grade fluid with adiabatic free surface down an inclined plane," *Applied Mathematics and Mechanics*, vol. 30, no. 3, pp. 373–380, 2009.